




CDF-S XT1 and XT2: White Dwarf Tidal Disruption Events by Intermediate-mass Black Holes?

Zong-Kai Peng^{1,2}, Yi-Si Yang^{1,2}, Rong-Feng Shen³ , Ling-Jun Wang⁴, Jin-Hang Zou⁵, and Bin-Bin Zhang^{1,2,6}

¹School of Astronomy and Space Science, Nanjing University, Nanjing 210093, People's Republic of China; bbzhang@nju.edu.cn

²Key Laboratory of Modern Astronomy and Astrophysics (Nanjing University), Ministry of Education, Nanjing, People's Republic of China

³School of Physics & Astronomy, Sun Yat-Sen University, Zhuhai 519082, People's Republic of China; shenrf3@mail.sysu.edu.cn

⁴National Astronomical Observatories, Chinese Academy of Sciences, Beijing 100012, People's Republic of China

⁵Department of Space Sciences and Astronomy, Hebei Normal University, Shijiazhuang 050024, People's Republic of China

⁶Department of Physics and Astronomy, University of Nevada, Las Vegas, NV 89154, USA

Received 2019 August 8; revised 2019 September 16; accepted 2019 September 25; published 2019 October 14

Abstract

Recently, two fast X-ray transients (XT1 and XT2) have been reported from the search in the *Chandra* Deep Field (CDF) data. Each transient shows an initial plateau lasting around hundreds to thousands of seconds followed by a rapid decay in the light curve. In particular, CDF-S XT2 is found to be associated with a galaxy at redshift $z = 0.738$ and was explained as a counterpart of a binary neutron-star merger event. In this Letter, motivated by the short duration and decay slopes of the two transients, we consider an alternative interpretation in which both events are accretion-driven flares from tidal disruption of white dwarfs by intermediate-mass black holes. We derive a theoretical model of the accretion rate history and find that it fits the observed X-ray light curves well. The extremely super-Eddington peak luminosity of XT2 can be explained by the beaming effect of the system, likely in the form of a jet.

Unified Astronomy Thesaurus concepts: [Intermediate-mass black holes \(816\)](#); [Tidal disruption \(1696\)](#); [White dwarf stars \(1799\)](#); [X-ray transient sources \(1852\)](#)

1. Introduction

The physical process of the tidal disruption event (TDE), which happens when a star is disrupted by a black hole (BH), has been investigated by many authors (Hills 1975; Lacy et al. 1982; Carter & Luminet 1983; Rees 1988; Evans & Kochanek 1989). The radiation of TDEs ranges from optical to X-ray energy bands. Dai et al. (2018) proposed a unified model of TDE and pointed out that the different emission may be caused by the different viewing angles. Dai et al. (2018) also studied the disk dynamics of the TDE through general relativistic radiation magnetohydrodynamic simulations and proposed that a jet can be produced. If a jet does exist in a TDE, the observations would be subject to the beaming effect. Some recent TDE observations indeed suggest the existence of a jet component (Bloom et al. 2011; Cenko et al. 2012; Brown et al. 2015). When a main-sequence star is disrupted by a BH, the process will last for years. However, the timescale will be much shorter if the disrupted object is a compact star such as a white dwarf (WD; Krolik & Piran 2011; Haas et al. 2012; Lodato 2012; Kawana et al. 2018). In the case of a WD-involved TDE, the BH mass cannot exceed $\sim \text{few} \times 10^5 M_\odot$ (hence, a stellar-mass BH or an intermediate-mass BH); otherwise, the WD is swallowed as a whole and there will be no observed emission (Clausen et al. 2012; Kawana et al. 2018).

Since the Laser Interferometer Gravitational-Wave Observatory (LIGO) and Virgo discovered the first gravitational-wave (GW) event GW150914 (Abbott et al. 2016a, 2016b), stellar-mass ($\sim 10 M_\odot$) BHs are realized to be common in the universe. Meanwhile, mounting evidence shows that supermassive BHs ($> 10^6 M_\odot$) exist at the centers of most galaxies (Kormendy & Richstone 1995). The origin of intermediate-mass BHs (IMBHs), on the other hand, remains an open question and some recent observations suggest they do exist in the centers of

dwarf galaxies or star clusters (Farrell et al. 2009; Chilingarian et al. 2018; Lin et al. 2018).

Recently, two fast X-ray transients from the 7 Ms *Chandra* Deep Field-Source survey, namely, CDF-S XT1 (Bauer et al. 2017) and CDF-S XT2 (Xue et al. 2019), were reported. CDF-S XT1 seems to be associated with a faint galaxy without any spectroscopic redshift measurement.⁷ Xue et al. (2019) pointed out that CDF-S XT2 was associated with a galaxy at redshift 0.738 and lies in its outskirts with a moderate offset of $0''.44 \pm 0''.25$.

The light curve of CDF-S XT1 shows a rise within ~ 100 s to the peak flux of $F_{0.3-10 \text{ KeV}} \approx 5 \times 10^{-12} \text{ erg s}^{-1} \text{ cm}^{-2}$, then a power-law decay in hours with a slope of -1.53 ± 0.27 (Bauer et al. 2017). The light curve of CDF-S XT2 shows a long plateau, and then a sudden break at ~ 3000 s. Its peak luminosity between 0.3 and 10 KeV is $\approx 3 \times 10^{45} \text{ erg s}^{-1}$. For XT2, Xue et al. (2019) reported the best-fitting power-law indices of $-0.14^{+0.03}_{-0.03}$ and $-2.16^{+0.26}_{-0.29}$ before and after the break.

Without establishing a confirmed redshift (hence luminosity), there were several theoretical models to explain CDF-S XT1: an orphan afterglow of a short gamma-ray burst; a low-luminosity gamma-ray burst with a large redshift; or a TDE of IMBH with WD (Bauer et al. 2017). For CDF-S XT2, by considering its luminosity, host galaxy offset, and event rate, Xue et al. (2019) pointed out that it most likely originated from a magnetar that was formed after a binary neutron-star (NS) merger event, a possibility considered by Lü et al. (2019), Sun et al. (2019), and Xiao et al. (2019) as well, while other possibilities are not entirely ruled out.

The late temporal decay slope of CDF-S XT2 is steeper than the canonical value $-5/3$ of a stellar TDE's debris mass fallback rate (Rees 1988). In addition, we noticed that the

⁷ Bauer et al. (2017) pointed out a photometric redshift of 2.23 with large uncertainties.

timescale of CDF-S XT2 is much shorter than those of stellar TDEs, but it fits well the scenario of a WD-involved TDE. In this Letter we explore the tidal encountering process of a WD and an IMBH and its subsequent accretion as a possible origin of these two CDF-S transients. A similar scenario is considered by Shen (2019), who proposed a model that a WD is tidally stripped by an IMBH to explain two fast, ultraluminous X-ray bursts found by Irwin et al. (2016).

We describe the model in Section 2, paying particular attention to the role of the viscous disk accretion in shaping the light curve. The model prediction is then fitted to the observed light curve and the results are presented in Section 3. The discussion and conclusions are summarized in Section 4.

2. The Model

We aim to interpret CDF-S XT2 and XT1 as accretion transients resulted from a TDE of a WD encountering an IMBH. We consider that the WD approaches the IMBH on a parabolic orbit. When the WD reaches the tidal radius (Hills 1975; Rees 1988; Cannizzo et al. 1990; Kochanek 1994),

$$R_t \simeq R_* \left(\frac{M_{\text{BH}}}{M_*} \right)^{1/3}, \quad (1)$$

the surface material will be disrupted by BH, where M_{BH} is the mass of BH, and R_* and M_* are the radius and mass of the WD, respectively. We consider both cases of a full disruption and a partial disruption (“stripping”). For the tidal stripping case, a factor of 2 is introduced in front of R_* in Equation (1) (Shen 2019).

An analytical solution of the WD mass–radius relation was derived by Nauenberg (1972). By fitting to a simple power law, we find it can be roughly approximated by $R_*/R_\odot \simeq 0.0078 m_*^{-2/3}$ for the mass range $0.2 < m_* < 1.2$, where $m_* = M_*/M_\odot$ with M_\odot being solar mass and R_\odot being solar radius. This approximation serves to ease our analysis of parameter dependence later. Substituting R_* in Equation (1), we have

$$R_t \simeq 18 \left(\frac{M_\odot}{M_*} \right) \left(\frac{10^3 M_\odot}{M_{\text{BH}}} \right)^{2/3} R_S, \quad (2)$$

where R_S is the Schwarzschild radius of the BH.

Similar to the stellar TDE case, the bound portion of the disrupted WD material falls back to the disruption site with a mass rate history of

$$\dot{m}_{\text{fb}}(t) = \frac{\Delta m}{t_{\text{fb}}} \frac{(n-1)}{n} f(t/t_{\text{fb}}), \quad (3)$$

where

$$f(x) = \begin{cases} 1, & \text{for } x \leq 1, \\ x^{-n}, & \text{for } x > 1. \end{cases} \quad (4)$$

Here Δm is the total bound mass and $n = 5/3$ for typical TDEs. The timescale over which the bulk of the debris stream falls back is

$$t_{\text{fb}} = \frac{\pi R_t^3}{\sqrt{2GM_{\text{BH}}R_*^3}} \simeq 77 \left(\frac{M_{\text{BH}}}{10^3 M_\odot} \right)^{1/2} \left(\frac{M_\odot}{M_*} \right)^2 \text{ s}, \quad (5)$$

where the last step uses Equation (1) and the WD’s mass–radius relation. After a time of t_{fb} , the fallback rate drops as

$\propto t^{-5/3}$. In the above calculation, $t = 0$ is set to the epoch when the first parcel of disrupted material falls back to the disruption site.

The returned mass cannot be digested promptly by the BH. After forming a disk, it will swirl inward within the disk. This process can be accounted for by a viscous accretion timescale $t_{\text{acc}}(R_t)$; it is the time that each parcel of mass has to spend before reaching the BH. It depends on the tidal radius R_t —where the disrupted material first returns to, and on the physical regimes of the disk as in

$$t_{\text{acc}}(R_t) = \frac{1}{\alpha} \sqrt{\frac{R_t^3}{GM}} \left(\frac{H}{R} \right)^{-2} \\ \simeq 23 m_*^{-1} \left(\frac{0.1}{\alpha} \right) \left(\frac{H}{R} \right)^{-2} \text{ s}, \quad (6)$$

where α is the viscosity parameter (Shakura & Sunyaev 1973; Frank et al. 2002), and H/R is the disk thickness-to-radius ratio. The last step of Equation (6) utilized Equation (1) and the WD mass–radius relation. It shows that t_{acc} is insensitive to the BH mass M , though H/R may contain a subtle M -dependence.

If the disk is in the radiatively efficient and geometrically thin regime (i.e., Shakura & Sunyaev disk), $H/R \approx 0.01 \dot{m}^{1/5} (\alpha M_4)^{-1/10} r^{1/20}$, where \dot{m} and r are the accretion rate and disk radius *normalized* by $L_{\text{Edd}}/(0.1c^2)$ and R_S , respectively (Kato et al. 2008). If the disk is in the advective-cooling dominated and geometrically thick regime (i.e., slim disk; Abramowicz et al. 1988), H/R is approximately unity. The borderline between the two regimes is $\dot{m} \sim r/10$. In any case, $t_{\text{acc}}(R_t)$ ranges from $\sim 10^2$ s to $\sim 10^5$ s given $0.01 \leq H/R \leq 1$.

With a mass supplied from fallback and a drain due to accretion, the global temporal evolution of the disk can be written as

$$\frac{dm_d}{dt} = \dot{m}_{\text{fb}}(t) - \dot{m}_{\text{acc}}(t), \quad (7)$$

and the accretion rate can be approximately expressed as

$$\dot{m}_{\text{acc}}(t) = \frac{m_d}{t_{\text{acc}}(R_t)}. \quad (8)$$

A general solution of $m_d(t)$ to Equation (7) can be obtained in a time-integrated form (Kumar et al. 2008). Since t_{acc} can be roughly regarded as a constant as all disrupted material returns to the same radius, the accretion rate history can be solved as

$$\dot{m}_{\text{acc}}(t) = \frac{1}{t_{\text{acc}}} \int_0^t \dot{m}_{\text{fb}}(t') \exp\left[-\frac{(t-t')}{t_{\text{acc}}}\right] dt'. \quad (9)$$

Combining Equations (3)–(4) and (9), the solution can be rewritten as

$$\dot{m}_{\text{acc}}(t) = \frac{\Delta m}{t_{\text{acc}}} A(t, t_{\text{fb}}, t_{\text{acc}}, n), \quad (10)$$

where, with given parameters t_{fb} , t_{acc} and n , the function

$$A(t, t_{\text{fb}}, t_{\text{acc}}, n) = \frac{n-1}{n} \\ \times \int_0^{t/t_{\text{fb}}} f(t'/t_{\text{fb}}) \exp\left[-\frac{(t-t')}{t_{\text{acc}}}\right] d(t'/t_{\text{fb}}) \quad (11)$$

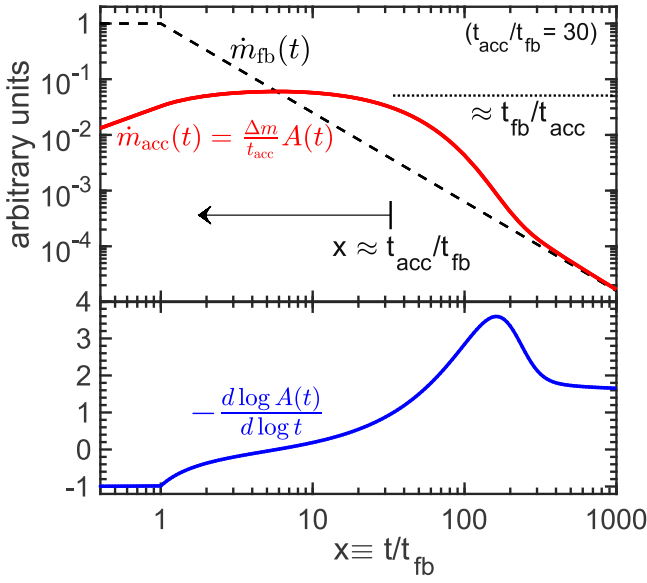


Figure 1. An example of the accretion rate history (red solid line) calculated from Equation (10) for a given mass fallback rate history (black dashed line; Equation (3)). The lower panel plots the instantaneous temporal slope of the accretion rate.

contains all the temporal shape information of $\dot{m}_{\text{acc}}(t)$ and its peak value is ~ 1 .

Figure 1 shows an example of the shape of the accretion rate history $\dot{m}_{\text{acc}}(t)$. Compared with the short-duration, fast-decaying mass supply curve $\dot{m}_{\text{fb}}(t)$, the accretion rate shows a “slowed” plateau, followed by a steep drop toward the decaying tail of the supply rate. The duration of the plateau is $\approx t_{\text{acc}}$, and the level of the plateau, or the peak accretion rate, is $\approx \Delta m / t_{\text{acc}}$. The post-plateau drop is not possessed of an asymptotic slope (not until $t \gg t_{\text{acc}}$), unlike the case of the spin-down power rate of a young pulsar. However, its instantaneous slope (shown in the lower panel) is certainly steeper than n and is $\approx 2-3$. As will be shown below, such values are consistent with the observed slope of CDF-S XT1 and XT2.

Introducing a constant radiative efficiency η , we calculate the bolometric luminosity light curve from the accretion rate history:

$$L(t) = \eta \dot{m}_{\text{acc}}(t) c^2 = \eta c^2 \frac{\Delta m}{t_{\text{acc}}} A(t, t_{\text{fb}}, t_{\text{acc}}, n). \quad (12)$$

For CDF-S XT2, its luminosity is $\sim 10^{45}$ erg s $^{-1}$, and the duration of the plateau of the light curve is ≈ 3000 s. So we

have

$$L(t) = 6 \times 10^{44} \left(\frac{\eta}{0.1} \right) \left(\frac{\Delta m}{10^{-5} M_{\odot}} \right) \times \left(\frac{3000 \text{ s}}{t_{\text{acc}}} \right) A(t, t_{\text{fb}}, t_{\text{acc}}, n) \text{ erg s}^{-1}. \quad (13)$$

3. The Fit

We fit the light curve of CDF-S XT2 using Equation (13) with three free parameters: t_{acc} , t_{fb} , and $\delta = \log(\eta \Delta m / M_{\odot})$, the last of which is introduced in recognition of the degeneracy between Δm and η ; n is fixed to $5/3$. Using a Monte Carlo (MC) fitting tool developed by us (Zhang et al. 2015), we get the best-fitting parameters listed in Table 1.

The goodness of the fit meets the condition $\chi^2 = 11.71 < \chi^2_{\alpha=0.05, \text{DOF}=8} = 15.51$, suggesting that the fit is acceptable at the 0.05 significance level. The parameter constraints as well as the best-fit model curves are presented in Figure 2. While δ and t_{acc} are constrained reasonably well, we found t_{fb} is not sensitive in our fit but is consistent with a small value in the parameter space. A small t_{fb} might be caused by a large WD mass (see Equation (5)).

The latest two data points of XT2 seem to show a slightly shallower decay than the model predicted. We find that if we adjust the value of n to 1.5 or 1.3, these two data points fit better and the overall goodness of fitting is improved. Although some numerical simulations of partial disruptions (Guillochon & Ramirez-Ruiz 2013; Coughlin & Nixon 2019) or those taking into account some realistically evolved stellar structures (Golightly et al. 2019; Law-Smith et al. 2019) tend to find the n that are steeper than $5/3$, so far in the TDE literature there has been no finding that $n < 5/3$. On the other hand, the simulations mentioned above are all about disruptions of normal stars. For disruptions of compact stars like WDs considered here, could it be $n < 5/3$? It is an interesting question for future numerical exploration.

Similarly, we fit the light curve of CDF-S XT1 with the same approach. We use one free parameter f_0 to account for η , Δm , and the unknown redshift z . So the observed flux light curve can be written as

$$F(t) = f_0 \times \left(\frac{100 \text{ s}}{t_{\text{acc}}} \right) A(t, t_{\text{fb}}, t_{\text{acc}}, n) \text{ erg cm}^{-2} \text{ s}^{-1}. \quad (14)$$

Figure 3 shows the fitting to the light curve of XT1 and the parameter corner.

The XT1 fit yields a $\chi^2 = 11.48$, which is $< \chi^2_{\alpha=0.05, \text{DOF}=6} = 12.59$, indicating the fit is still acceptable at the 0.05 significance level. The second and third data points contribute most of the residuals after the fit, which we interpret

Table 1
Best-fitting Parameters from MCMC Code

Parameters	δ^a	f_0^b	$t_{\text{acc}}(\text{s})$	$t_{\text{fb}}(\text{s})$	Chisq/dof
XT1	...	$-10.6^{+0.04}_{-0.06}$	$70.59^{+110.04}_{-24.91}$	$271.35^{+103.44}_{-104.79}$	11.48/6.0
XT2	$-5.72^{+0.04}_{-0.05}$...	$1523.90^{+138.31}_{-264.05}$	$6.70^{+34.66}_{-6.60}$	11.71/8.0

Notes.

^a Because the stripped mass Δm and η are degenerated with each other, we combined them into one single parameter $\delta = \log\left(\eta * \frac{\Delta m}{M_{\odot}}\right)$.

^b The redshift of CDF-S XT1 is not given, so we combined redshift z , η , and Δm into one parameter f_0 .

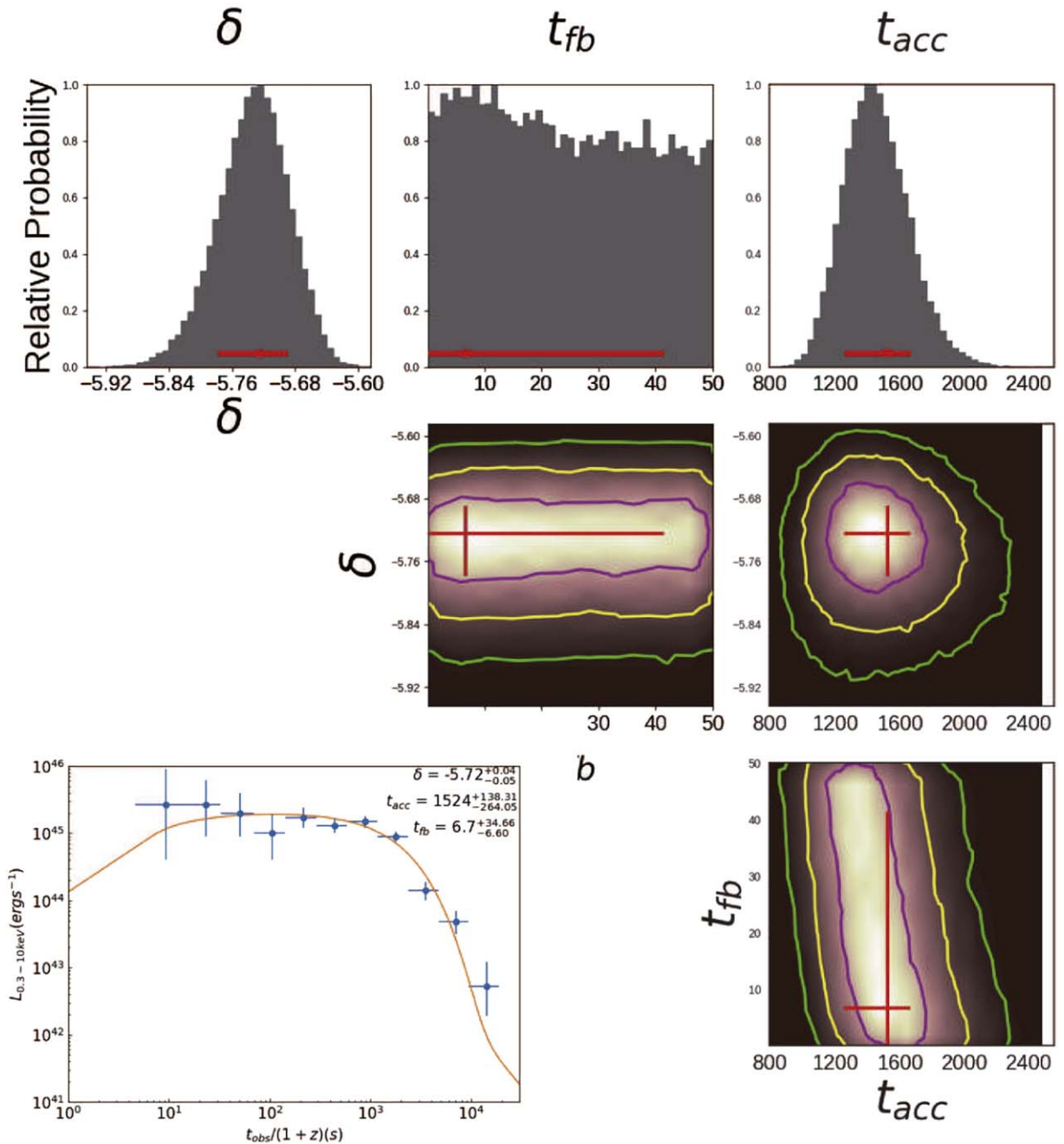


Figure 2. Fitting our TDE model to the observed data of CDF-S XT2. The bottom left plot shows the best-fit modeled light curves (solid line) overlapped on the observed data points (filled circles). Top right corner plot shows the constraints of the three best-fit parameters.

as being due to some early fast variabilities of the jet luminosity.

Compared with XT2, a shorter duration of the plateau of XT1 leads to a shorter accretion timescale. The best fit of XT1 gives $t_{fb} \simeq 271$ s and $t_{acc} \simeq 71$ s. Those values are consistent with the estimation using Equations (5) and (6). The relatively small t_{acc} indicates $H/R \sim 1$ (thus, a slim disk), which is consistent with a super-Eddington accretion case (Abramowicz et al. 1988; Dotan & Shaviv 2011).

4. Discussion and Conclusions

Motivated by the short timescales and high luminosities of two recently discovered X-ray transients CDF-S XT1 and XT2,

we calculate the light curve of an accretion-driven transient when a WD is tidally disrupted by an intermediate-mass BH. We find that the model fits well to both events. A similar model has been used to explain some ultraluminous X-ray bursts (Shen 2019). By introducing a viscous accretion timescale, this model has more flexibility in explaining the temporal behavior of a light curve than the conventional stellar TDE model. For example, the late-time slope of XT2 is ≈ -2.1 , which is steeper than those of other typical TDEs (Lacy et al. 1982; Rees 1988; Li et al. 2002), but it can be well accounted for using Equations (13)–(14). The mass of the central black hole in our model is also flexible, but recent observations (e.g., 3XMM J215022.4-055108; Lin et al. 2018) suggest IMBHs may be

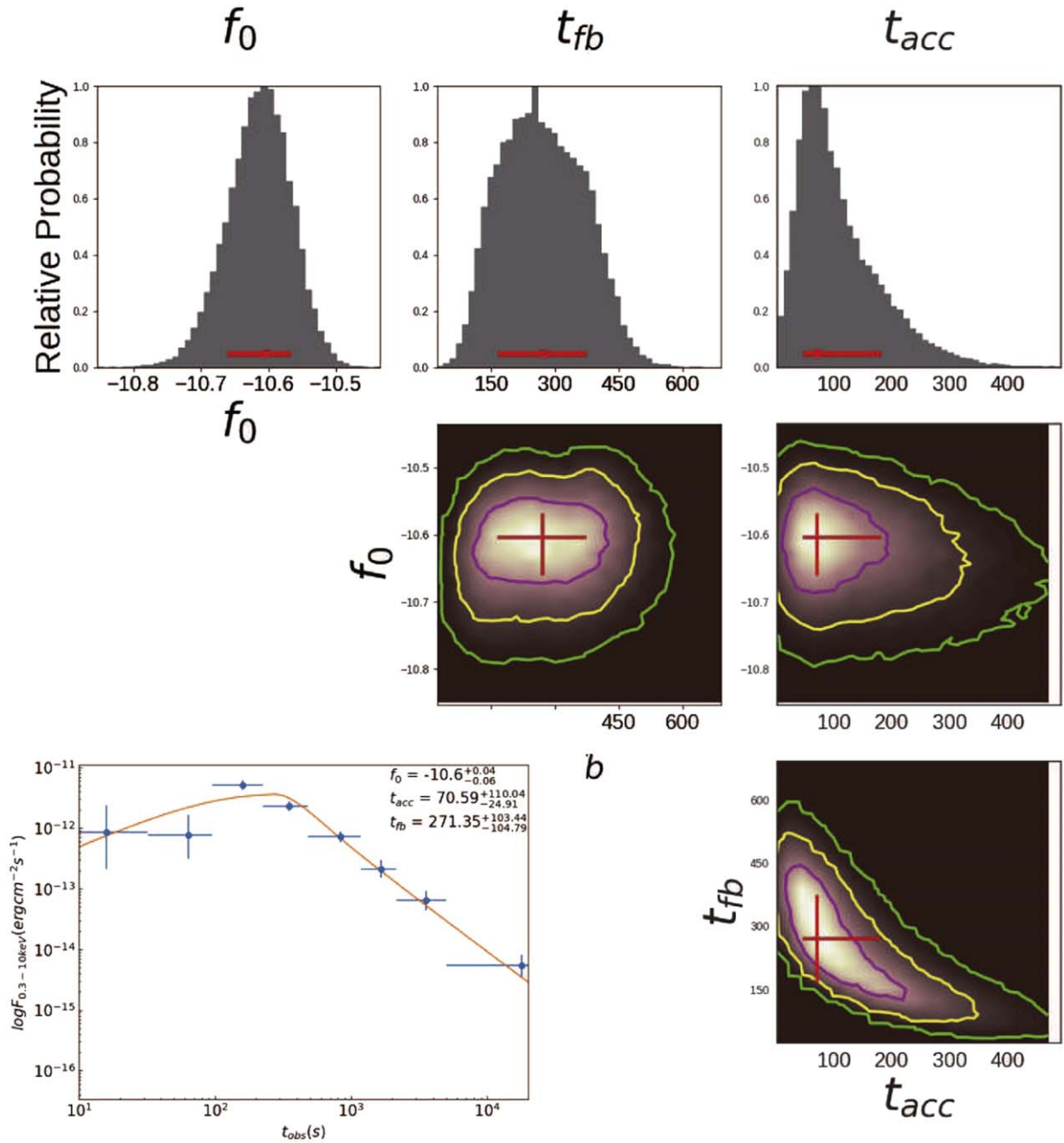


Figure 3. Same as Figure 3, but for the fit of CDF-S XT1. The fitting model is described in Equation (14). The f_0 is logarithmic.

common in off-center star clusters that may fit in well with the central object in our model.

For a WD approaching the BH, three possible types of orbits are permitted, namely, elliptical, parabolic, and hyperbolic (Li et al. 2002; Kobayashi et al. 2004). If the orbit is elliptical, a periodicity of the light curve is expected, which is not observed. This may suggest that the orbit is parabolic or hyperbolic for XT1 and XT2.

Comparing the best-fit results of CDF-S XT1 with CDF-S XT2 in Table 1, we notice that t_{fb} of CDF-S XT2 is shorter, but its t_{acc} is longer. This suggests that, if the BH masses in the two systems are the same, the WD in the case of XT2 might be heavier (i.e., more compact), so its disruption radius is closer to the BH (see Equation (5)). The longer t_{acc} in XT2 is likely due to a lower disk thickness ratio H/R because the latter carries the

most sensitive parameter dependence in Equation (6). A lower H/R in turn might be caused by a lower Eddington-normalized accretion rate. This could suggest that XT2 was a tidal stripping event because the total bound mass Δm can be much smaller than that of a full disruption event.

The isotropic-equivalent peak luminosity of CDF-S XT2, $\approx 3 \times 10^{45} \text{ erg s}^{-1}$, is extremely high, which raises the possibility of a relativistically beamed emission. Three relativistic jetted TDE candidates have been discovered so far: Sw J1644+57 (Bloom et al. 2011; Burrows et al. 2011), Sw J2058+0516 (Cenko et al. 2012; Pasham et al. 2015), and Sw J1112–8238 (Brown et al. 2015). The 2D model of Dai et al. (2018) suggests that the X-ray emission of TDEs may be caused by jets through the Blandford–Znajek process.

Similarly, the WD–IMBH tidal disruption/stripping discussed here may produce a jet as well.

Xue et al. (2019) estimated the CDF-S XT2-like event rate density to be $1.3_{-1.1}^{+2.8} \times 10^4 \text{ Gpc}^{-3} \text{ yr}^{-1}$. For CDF-S XT1, Bauer et al. (2017) estimated a large range of the event rate, $\sim 10^3 \text{ Gpc}^{-3} \text{ yr}^{-1}$ for $z = 0.5$ to $\sim 1 \text{ Gpc}^{-3} \text{ yr}^{-1}$ for $z = 3$.

Theoretically, the rates of WD disruptions are very uncertain. For IMBHs in globular clusters (GCs), Baumgardt et al. (2004) estimated a total stellar TDE rate of $\sim 10^{-7} \text{ yr}^{-1}$ via N -body simulations of GCs with an initial central BH mass of $10^3 M_{\odot}$. Among the disrupted stars, $\sim 15\%$ are WDs, giving a rate of $\sim 1.5 \times 10^{-8} \text{ yr}^{-1}$. Adopting a number density of 34 Mpc^{-3} of GCs, this gives a volumetric rate of $R_{\text{IMBH-WD}} \sim 500 \text{ yr}^{-1} \text{ Gpc}^{-3}$ (Haas et al. 2012; Shcherbakov et al. 2013). Recently, Fragione et al. (2018) semianalytically calculated the evolution of a population of GCs in a galaxy and found a rate of WD TDE $\sim 10^{-5} \text{ yr}^{-1}$ per galaxy; combining this with GC population's dependence on redshift and galaxy types, their results show a present-day volumetric rate of $R_{\text{IMBH-WD}} \sim 10 \text{ yr}^{-1} \text{ Gpc}^{-3}$.

For IMBHs in dwarf galaxies, MacLeod et al. (2014) calculated a rate of $\sim 10^{-6} \text{ yr}^{-1}$ per IMBH for WD disruptions via the loss-cone dynamics for the BH mass range of 10^4 – $10^5 M_{\odot}$. This rate is ~ 30 times lower than that of main-sequence stellar TDEs by supermassive black holes (e.g., Stone & Metzger 2016). Assuming a number density of dwarf galaxies $\sim 10^7 \text{ Gpc}^{-3}$ (Shcherbakov et al. 2013; MacLeod et al. 2014) and an occupation fraction f_{IMBH} of IMBHs in dwarf galaxies, then the volumetric rate is $R_{\text{IMBH-WD}} \sim 10 f_{\text{IMBH}} \text{ yr}^{-1} \text{ Gpc}^{-3}$.

Compared with WD–IMBH TDEs, a similar case that happens more commonly is the tidal disruption/stripping of MS stars by IMBHs. Indeed, as was shown in Fragione et al. (2018), the event rate of MS–IMBH TDEs is about 30 times higher than that of WD–IMBH TDEs in most galaxies. However, the timescale (\sim years) of MS–IMBH TDEs is much longer than that of WD–IMBH TDEs (\sim hours; Chen & Shen 2018), which might disguise themselves as persisting sources, thus hindering the identification of their transient nature. For disruptions of evolved stars like giants, the corresponding timescales are even longer (~ 10 times; MacLeod et al. 2012). From the timescale consideration, XT1 and XT2 are unlikely to be MS TDEs. Chen & Shen (2018) predicted a detection rate of 20 MS–IMBH TDEs per year by Zwicky Transient Factory, and 0.03 yr^{-1} by *Chandra*. Lin et al. (2018) reported an MS–IMBH TDE candidate 3XMM J215022.4–055108, from which they inferred the event rate of 3XMM J215022.4–055108-like TDEs to be $\sim 10 \text{ Gpc}^{-3} \text{ yr}^{-1}$. This low detection rate may suggest that most of the MS–IMBH TDEs might have been missed due to their slow-evolution disguise.

Future detection of more similar events might either rule out the model presented here for those events or clear up our current ignorance about the IMBH demographics.

B.B.Z. thank the hospitality of X. Liu during the visit at Xinjiang Observatory and the support by the National Key R&D Program of China under grant No. 2018YFA0404602. This work is also supported by the National Key Research and Development Program of China (2018YFA0404204) and NSFC-11833003. R.-F.S. is supported by NSFC grant 11673078. L.J.W. acknowledges the support from the National

Program on Key Research and Development Project of China (grant 2016YFA0400801). We thank Bing Zhang for helpful discussions and the anonymous referee for helpful suggestions.

ORCID iDs

Rong-Feng Shen  <https://orcid.org/0000-0001-5012-2362>

References

- Abbott, B. P., Abbott, R., Abbott, T. D., et al. 2016a, *PhRvL*, **116**, 131102
 Abbott, B. P., Abbott, R., Abbott, T. D., et al. 2016b, *PhRvL*, **116**, 061102
 Abramowicz, M. A., Czerny, B., Lasota, J. P., & Szuszkiewicz, E. 1988, *ApJ*, **332**, 646
 Bauer, F. E., Treister, E., Schawinski, K., et al. 2017, *MNRAS*, **467**, 4841
 Baumgardt, H., Makino, J., & Ebisuzaki, T. 2004, *ApJ*, **613**, 1143
 Bloom, J. S., Giannios, D., Metzger, B. D., et al. 2011, *Sci*, **333**, 203
 Brown, G. C., Levan, A. J., Stanway, E. R., et al. 2015, *MNRAS*, **452**, 4297
 Burrows, D. N., Kennea, J. A., Ghisellini, G., et al. 2011, *Natur*, **476**, 421
 Cannizzo, J. K., Lee, H. M., & Goodman, J. 1990, *ApJ*, **351**, 38
 Carter, B., & Luminet, J.-P. 1983, *A&A*, **121**, 97
 Cenko, S. B., Krimm, H. A., Horesh, A., et al. 2012, *ApJ*, **753**, 77
 Chen, J.-H., & Shen, R.-F. 2018, *ApJ*, **867**, 20
 Chilingarian, I. V., Katkov, I. Yu., Zolotukhin, I. Yu., et al. 2018, *ApJ*, **863**, 1
 Clausen, D., Eracleous, M., Sigurdsson, S., & Irwin, J. A. 2012, *EPJ Web Conf.*, **39**, 01005
 Coughlin, E. R., & Nixon, C. J. 2019, *ApJL*, **883**, L17
 Dai, L., McKinney, J. C., Roth, N., Ramirez-Ruiz, E., & Miller, M. C. 2018, *ApJL*, **859**, L20
 Dotan, C., & Shaviv, N. J. 2011, *MNRAS*, **413**, 1623
 Eggleton, P. P. 1983, *ApJ*, **268**, 368
 Evans, C. R., & Kochanek, C. S. 1989, *ApJL*, **346**, L13
 Farrell, S. A., Webb, N. A., Barret, D., Godet, O., & Rodrigues, J. M. 2009, *Natur*, **460**, 73
 Fernández, R., Margalit, B., & Metzger, B. D. 2019, *MNRAS*, **488**, 259
 Fragione, G., Leigh, N. W. C., Ginsburg, I., & Kocsis, B. 2018, *ApJ*, **867**, 119
 Frank, J., King, A., & Raine, D. J. 2002, in *Accretion Power in Astrophysics*, ed. J. Frank, A. King, & D. Raine (Cambridge: Cambridge Univ. Press), 398
 Golightly, E. C. A., Nixon, C. J., & Coughlin, E. R. 2019, *ApJL*, **882**, L26
 Guillochon, J., & Ramirez-Ruiz, E. 2013, *ApJ*, **767**, 25
 Haas, R., Shcherbakov, R. V., Bode, T., & Laguna, P. 2012, *ApJ*, **749**, 117
 Hills, J. G. 1975, *Natur*, **254**, 295
 Irwin, J. A., Maksym, W. P., Sivakoff, G. R., et al. 2016, *Natur*, **538**, 356
 Kato, S., Fukue, J., & Mineshige, S. 2008, *Black Hole Accretion Disks* (Kyoto: Kyoto Univ. Press)
 Kawana, K., Tanikawa, A., & Yoshida, N. 2018, *MNRAS*, **477**, 3449
 Kobayashi, S., Laguna, P., Phinney, E. S., & Mészáros, P. 2004, *ApJ*, **615**, 855
 Kochanek, C. S. 1994, *ApJ*, **422**, 508
 Kormendy, J., & Richstone, D. 1995, *ARA&A*, **33**, 581
 Krolik, J. H., & Piran, T. 2011, *ApJ*, **743**, 134
 Kumar, P., Narayan, R., & Johnson, J. L. 2008, *MNRAS*, **388**, 1729
 Lacy, J. H., Townes, C. H., & Hollenbach, D. J. 1982, *ApJ*, **262**, 120
 Law-Smith, J., Guillochon, J., & Ramirez-Ruiz, E. 2019, *ApJL*, **882**, L25
 Li, L.-X., Narayan, R., & Menou, K. 2002, *ApJ*, **576**, 753
 Lin, D., Strader, J., Carrasco, E. R., et al. 2018, *NatAs*, **2**, 656
 Lloyd-Ronning, N. M., Dolence, J. C., & Fryer, C. L. 2016, *MNRAS*, **461**, 1045
 Lodato, G. 2012, *EPJ Web Conf.*, **39**, 01001
 Lodato, G., Franchini, A., Bonnerot, C., & Rossi, E. M. 2015, *JHEAp*, **7**, 158
 Lü, H.-J., Yuan, Y., Lan, L., et al. 2019, arXiv:1904.06664
 MacLeod, M., Goldstein, J., Ramirez-Ruiz, E., Guillochon, J., & Samsing, J. 2014, *ApJ*, **794**, 9
 MacLeod, M., Guillochon, J., & Ramirez-Ruiz, E. 2012, *ApJ*, **757**, 134
 Nauenberg, M. 1972, *ApJ*, **175**, 417
 Paczyński, B. 1971, *ARA&A*, **9**, 183
 Pasham, D. R., Cenko, S. B., Levan, A. J., et al. 2015, *ApJ*, **805**, 68
 Rees, M. J. 1988, *Natur*, **333**, 523
 Shakura, N. I., & Sunyaev, R. A. 1973, *A&A*, **24**, 337
 Shcherbakov, R. V., Pe'er, A., Reynolds, C. S., et al. 2013, *ApJ*, **769**, 85
 Shen, R.-F. 2019, *ApJL*, **871**, L17
 Stone, N. C., & Metzger, B. D. 2016, *MNRAS*, **455**, 859
 Sun, H., Li, Y., Zhang, B., et al. 2019, arXiv:1908.01107
 Xiao, D., Zhang, B.-B., & Dai, Z.-G. 2019, *ApJL*, **879**, L7
 Xue, Y. Q., Zheng, X. C., Li, Y., et al. 2019, *Natur*, **568**, 198
 Zhang, B.-B., van Eerten, H., Burrows, D. N., et al. 2015, *ApJ*, **806**, 15